Here comes the hammer: sheet objects from the Cenote Sagrado, Chichén Itzá

José Luis Ruvalcaba Sil, Bryan Cockrell, Edith Ortiz Díaz

ABSTRACT: A multi-stage archaeometric analysis was undertaken of 22 hammered metals recovered from the Cenote Sagrado at Chichén Itzá, Mexico. These objects include sandals, axe-monies and tweezers. All metals were examined with optical microscopy (vis-UV-IR) for comprehensive documentation and with pXRF for determination of bulk composition. Finer resolution analyses, including RBS, SR-XRD and SR-XRF, were conducted on particular objects. Eighteen objects are Cu-Au-based, while the axe-monies and tweezers are Cu-based. At least two sandals were finished with electrochemical replacement gilding. Secondary alterations to the metals, from indentations to wrinkles, suggest that the objects were re-fabricated over time. The presence of particular compositions and fabrication techniques indicates that objects continued to be deposited in the Cenote several centuries after the main occupation of Chichén Itzá (AD 750-1050).

Introduction

Chichén Itzá was a major Maya political centre from AD 750 to 1050 (Fig 1). The site, along with adjacent town of Pisté, continues to be home to a Maya community today (Breglia 2005). Chichén Itzá, whose rise spurred the growth of the coastal port site of Isla Cerritos, was part of a commercial network that connected it to west and central Mexico and Guatemala, especially indexed by

Figure 1: Map showing the key sites and regions mentioned.

Figure 2: A view of the Cenote in 2010.

the sources of its obsidian, and to the Caribbean (Cobos 1998; 2010). The Cenote Sagrado is a water-filled limestone sinkhole, a common geological feature of Yucatán, at the northern end of Chichén Itzá in which many objects had been deliberately deposited in the past (Fig 2). Two major projects in the 20th century recovered metals along with jade, ceramics and various organic materials from the Cenote: Edward Thompson's dredging and diving project from 1904 to 1911, from which objects were sent to the Peabody Museum of Archaeology and

Ethnology (PMAE) and later to the Museo Nacional de Antropología (MNA) as part of exchanges, and the use of a pressurized airlift and divers by the Instituto Nacional de Antropología e Historia (INAH) in 1960-1961 and 1967-1968, from which objects were sent to the Museo Palacio Cantón (MPC). Both projects struggled with preservation of stratigraphy. The lack of metallurgical debris at Chichén Itzá and of ore and native metal in Yucatán suggest that the metal objects were imported to the Cenote.

Like the conspicuous loops on the metal bells (Cockrell *et al* 2015), the small circular and rectangular holes on the metal sheets from the Cenote suggest that many of the metals were once attached to other materials. The bells were suspended, swaying and emitting discordant sounds. The sheets were covering, concealing and presenting lustrous surfaces. Occasionally, the materials to which some sheets were connected, such as yucca fibre and wood, have been preserved with the metal. Otherwise, we only can surmise the variety of colours and textures that would have become apparent to participants in and observers of Cenote depositional events through the physical juxtaposition of different materials.

Sheet objects are less commonly recovered and/or reported than bells are in Mesoamerican archaeological contexts. Nevertheless, a wide array of sheet was recovered from the Cenote. On initial inspection, given the diversity of forms and surface appearances of the sheet specimens and the reality that sheet was manufactured in several regions of Mesoamerica (including western and southern Mexico and the Isthmian region – including present-day Panama and Costa Rica) (Camacho-Bragado *et al* 2005; Fleming 1992; Hosler 2009), we inferred that multiple metallurgical communities fabricated the sheet that was found.

Indicative of the insufficient documentation in Thompson's project is the identification of artefacts in the debris pile left by earlier excavators (Cirerol Sansores 1940). These artefacts included 'fragments of pure gold – rolled and stamped' [authors' translation]. To achieve limited stratigraphic control, Piña Chán (1970, 38) excavated the Cenote in quadrants and identified sheet metal (high-Au sheet and sandals) only in quadrant 3, where he also recovered rings and high-Au bells. Ceramics from the Cenote date to AD 800 to 1550 (Ball and Ladd 1992). In their chronologies, Coggins and Shane (1984) propose that sheet metal was deposited between the mid-8th century and the mid-12th century AD and that, later, objects covered with 'gold foil' were deposited from the mid-13th century AD to the Spanish invasion, while Piña Chán (1970, 56) includes metal sandals in an early depositional phase. We agree with these authors' proposal of successive depositions but seek to refine the chronological details.

Assemblage

Characterizations of 20 sheet objects, including six sandals (Fig 3), two axe-monies (Fig 4), two tubes (Fig 5) and ten objects that escape easy categorization, referred to here as 'ambiguous' (*eg* Fig 6), in the PMAE, MPC and MNA collections are presented. Two additional objects that are not sheets per se but were primarily hammered are also presented (Fig 7). They are a subset of the 148 Cenote metals from the museum collections that we have studied (Ortiz *et al* 2016). Our goal, in selecting the 75 hammered objects to study, and the 22 to present here (Table 1), was to show the diversity of

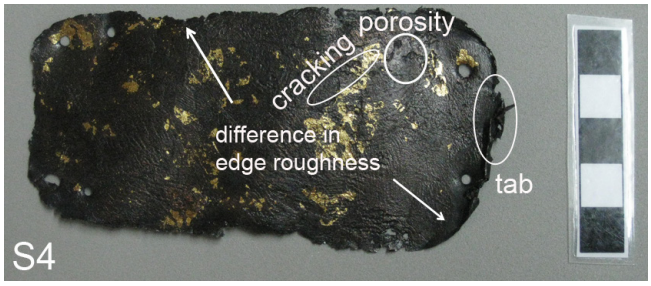

Figure 3: Sandal S4 with selected features noted. Scale bar 50mm.

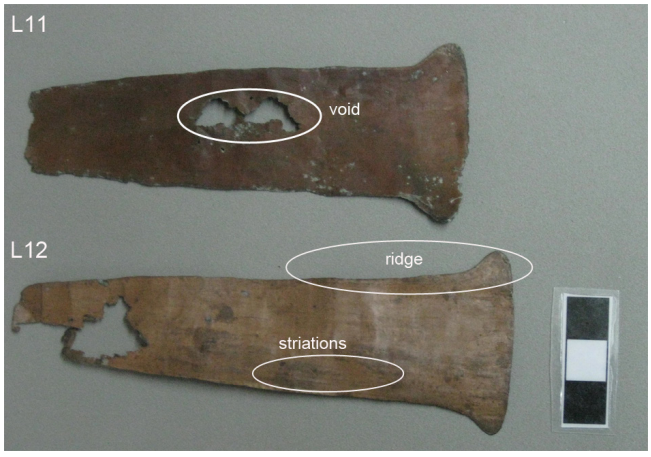

Figure 4: The axe-monies, L11 and L12, with selected features noted. Scale bar 30mm.

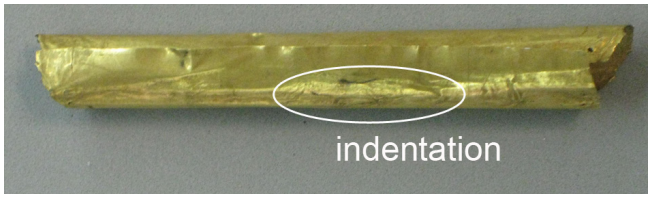

Figure 5: Tube L13 with selected features noted. Length 90mm.

Table 1: Hammered objects from Cenote Sagrado discussed in this paper.

					Technological traces			Consequences of fabrication				Secondary alteration				Other				
Object	Form	Museum	Additional analyses	Average thickness (mm)	Punched hole(s)	Embossed	Incised guideline(s)	Porosity	Extra metal	Ridges	Edges	Torn edges	Curled edges	Indentation	Wrinkle(s)	Crease(s)	Cracking	Void(s)	Incision(s)	Striation(s)	Discoloration(s)
L1	ambiguous	PMAE		0.05	x	x			Fine addition		smooth		x							x	x
L2	ambiguous	PMAE	RBS, SR-XRD, SR-XRF	0.13		x	x		Tab at edge	x	smooth	x	x		x						x
L3	ambiguous (once a tube or a cuff?)	PMAE	RBS, SR-XRD	0.02	x		x		Fine addition		varying	x				x	x				x
L4	ambiguous (once a cuff?)	PMAE		0.05	x		x				varying		x		x	x		x			x
L5	ambiguous	PMAE		0.05	x	x		Localised		x	rough		x							x	x
L6	ambiguous	PMAE		0.02							rough	x	x	x	x	x	x			x	x
L9	ambiguous (once a sandal?)	MPC		0.07		x					varying		x		x		x	x			
L10	sheet in form of serpent	MPC		0.20				Extensive			rough		x		x	x		x	x		x
L11*	axe-money	MPC		0.12						x	varying	x	x				x	x			x
L12*	axe-money	MPC		0.20			x			x	smooth	x			x	x		x		x	x
L13	tube (for beads?)	MNA		0.03	x		x				varying	x		x	x			x		x	x
L14	tube (for beads?)	MNA		0.01	x		x				varying	x			x					x	x
L15	ambiguous	MNA		0.01		x				x	smooth				x						x
L16	ambiguous	MNA		0.31					Fine addition	x	rough		x				x			x	x
S1	sandal	PMAE		0.24	x		x	Extensive			smooth								x		
S2	sandal	PMAE	RBS, SR-XRD, SR-XRF	0.24	x						varying								x		x
S3	sandal	PMAE	RBS, SR-XRD, SR-XRF	0.37	x			Extensive			smooth	x				x					x
S4	sandal	MPC		0.33	x			Extensive	Tab at edge		very rough		x				x				
S5	sandal	MPC		0.32	x			Extensive			varying		x						x		
S6	sandal	MNA		0.24	x			Extensive			varying						x		x		x
U2*	tweezers fragment	MPC		0.42							smooth						x	x	x	x	x
U3*	tweezers fragment	MPC		0.44							varying							x	x	x	x

Note: * indicates a copper alloy.

forms within the wider Cenote metal assemblage, with emphasis on forms that could not be categorized readily, but also to incorporate objects of similar forms across the three museum collections to ensure comparability.

Eighteen of the 22 are *tumbaga*, an alloy of Au, Ag and Cu that varies in fabrication technique and in cultural meaning in different ancient American contexts (Lechtman 2007, n.4).

Figure 6: Sheets of ambiguous form with selected features noted. Above, L3 with 20mm scale; below, L9 scale bar 50mm.

The four other objects discussed are Cu-based. In some cases, native or smelted metal would have been hammered and then chiselled with metal or stone to achieve an appropriate size for the sheet object, then hammered and potentially annealed to thickness and shape and possibly finished to convey a desired surface appearance to the metal. In most cases, native or smelted metal was alloyed before any hammering occurred. Embossing on five objects would have been undertaken with metal, stone and/or bone tools; the minimal depth of the embossed designs suggests to a smith today that a pitch-like foundation was not employed (B Heras pers comm). In this paper, we intend to draw attention to sheet, an overlooked class of metal in Mesoamerica, and evaluate materials whose 'function' is not immediately obvious. Three sheets appear to have lost significant corner portions (L9, L12, S5), while each of the two non-sheet objects (U2, U3) has a jagged edge that suggests they are fragments.

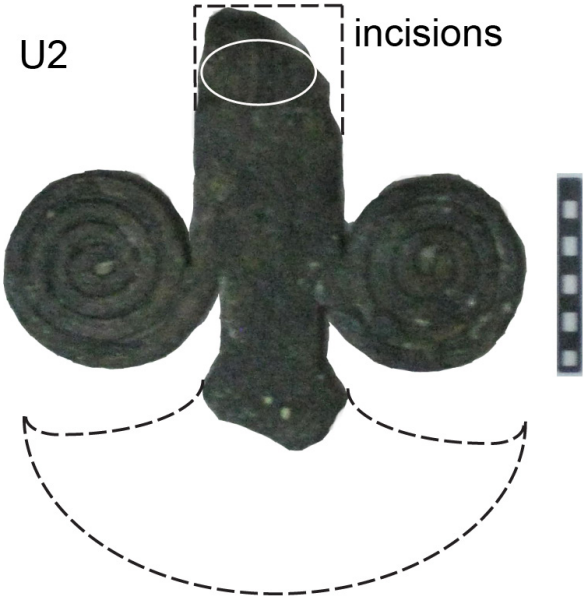

Figure 7: Tweezers fragment U2 with an outline of their presumed original appearance. Scale bar 10mm.

For all Cenote metals presented, we aim to:

- develop biographies of individual objects, drawing on multiple threads of data,
- identify particular technological styles (Lechtman 1984) within the assemblage based on the patterning across object biographies, and
- evaluate the metallurgical communities of practice (Lave and Wenger 1991) that these technological styles index through comparison with data from published metal corpora.

Previous analyses

Root (1937, 1946-7) analyzed Cenote sheets as early as 1927, employing gravimetry and Feré quartz spectrography. He analyzed at least five sandals, including S1 and S2. For sandal S1, there is a major discrepancy between his Ag concentration and that we identified and, for sandal S2, there is a minor difference between the Au concentrations (Table 2). These differences may arise from the different analytical methods and/or from compositional heterogeneity related to the metal's original fabrication, intentional surface treatments, natural corrosion and conservation.

Franco Velázquez and de Grinberg (2002) studied six Cenote bells, but not sheets, through visual inspection, energy dispersive X-ray fluorescence spectrometry (ED-XRF) and atomic absorption spectroscopy.

Contreras *et al* (2007) analyzed nine Cenote sheet specimens, including sandals. Comparing results of ED-XRF, scanning electron microscopy and particle-induced X-ray emission (PIXE)-Rutherford back-scattering spectroscopy (RBS) analysis for two sheet specimens – a sandal and an earflare, neither analyzed in the present project – they identified Au enrichment on both and inferred from the thickness of this enriched layer (0.4–0.5μm on the sandal and 0.3–0.4μm on the earflare) that electrochemical replacement gilding had been employed.

Methods

For all 148 objects analyzed, we:

- performed a visual observation of each metal with a magnifying glass, comparing the object to pre-existing typologies and taking measurements with callipers,
- documented the object with visible light microscopy for initial evaluation, ultraviolet (UV) microscopy for detection of organic residues and infrared (IR) microscopy for observation of tool impressions, and
- qualitatively characterized the elemental composition(s) with portable ED-XRF (pXRF).

In addition, three sheets were analyzed with synchrotron radiation-XRF (SR-XRF) to produce elemental distribution maps, four were analyzed with transmission synchrotron radiation-X-Ray Diffraction (SR-XRD) to determine the metal phases from crystalline structural data, and four sheets were analyzed with Rutherford backscattering spectroscopy (RBS) to create an elemental depth profile from the surface to the bulk. Full details of all the analytical methods and standards used are given in the Appendix.

Typology

Sheet objects receive little attention in published typologies of Mesoamerican metals. Bray (1977) states that the sandal form is unique to the Cenote Sagrado. The identification of six objects as sandals is aided by the preservation of a presumed ankle strap attached to one sandal (S1), joined to the sole by the tab-and-slot method. Owing to the recovery of textiles with shapes nearly identical to those of the metal sandals, it is assumed that the sandals were actually composite textile and metal objects. On at least one of the sandals (S4), textile impressions are preserved. Many of the more ambiguous forms of sheet may have been attached to wooden substrates. Potential analogues to some of these Cenote sheets are those Bray (1977) cites as 'sheet metal strip, foil, overlay or sheathing' from the sites of Mayapán, Zuuk, Nebaj, Chipal, Zaculeu, and Guaytan/S. Agustin Acasaguastlan as high-Au forms, and at Mayapán, El Cedral, Lamanai and Tajumulco as high-Cu forms. He also identifies 'diadems' from Iximché, 'plumes' and 'panaches' from the Cenote Sagrado and 'belts' and 'bracelets', both of which he only specifically ascribes to the Cenote but which he labels as 'widespread' in their distribution. Pendergast (1962) and Hosler (1988) present typologies of sheet objects but, in most cases, the forms do not appear in the excavated Cenote assemblage. The exceptions are the axe-monies mentioned but not illustrated by Hosler (1988); these objects receive more attention in Hosler *et al* (1990). Two Cenote sheet specimens (L11, L12) display formal similarities to Type 1a axe-monies fabricated in Guerrero, Michoacán and Oaxaca.

Metrics

Thickness was measured at between two and four points on individual objects, except for L15 (Fig 8). When thickness was below the detection limit of the callipers (0.01mm), the measurement was recorded as <0.01mm, and, for the purpose of calculations, it was treated as

Table 2: Comparison of the compositions of two sandals analysed by pXRF and the data for them obtained by Root (in Lothrop 1952 and PMAE archives).

Object	Analysis	Fe	Ni	Cu	Zn	As	Se	Ag	Sn	Sb	Pt	Au	Pb	Bi
S1	Root			L		T		L	S	T		S	S	X
	pXRF	t		M	t	t	ND	t	ND	ND	ND	m	ND	ND
S2	Root			95.9%				2%	0.1%			2%		
	pXRF	t	t	M	t	t	ND	t	ND	ND	ND	M	ND	ND

Notes: For pXRF analyses ND = not detected, M = major (≥10wt%), m = minor (10>x≥1wt%) and t = trace (<1wt%).
For Root's analyses L >20%, S = 1–20%, T = 0.01–1%. The meaning of X and blanks are unknown but the latter probably denote the element was not detected or was not tested for.

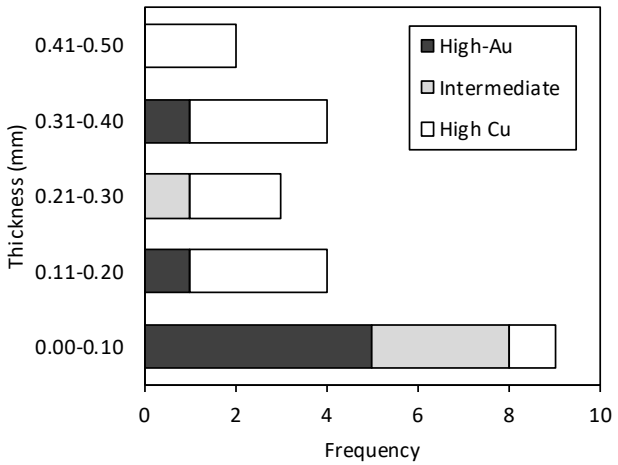

Figure 8: The thickness of the objects. High-Au = > 90wt% Au, Intermediate = 30–70wt% Au, High-Cu = >85wt% Cu.

0.01mm. The two thickest objects are the tweezers fragments. The average thickness of the high-Au objects (n=7) is 0.08mm (1σ=0.11mm, c_v=1.27), that of the high-Cu objects (n=11) is 0.27mm (1σ=0.12mm, c_v=0.44) and that of the objects of intermediate composition (n=4) is 0.08mm (1σ=0.11mm, c_v=1.39). While recognizing the high standard deviations for the thicknesses of the high-Au and intermediate metals, their lower average thickness, compared to the high-Cu objects, is conspicuous.

Five of the six sandals have an average maximum length of 144.20mm (1σ=18.26mm, c_v=0.13) and an average minimum width of 66.60mm (1σ=7.72mm, c_v=0.12). The sixth sandal is an outlier; its maximum length and width are less than half of those of the others. Potentially smiths designed it for an infant to wear and the others for adolescents and adults. Besides similarities in basic morphology, two object pairs (axe-monies L11, L12; hollow tubes L13, L14) each show striking similarity in their maximum lengths and widths.

Superficial features

Table 1 shows which features were noted on each object. They may represent:

- a 'technological decision' of the metalsmith(s);
- a 'consequence of fabrication' that the smith(s) did not intend;
- a 'secondary alteration' that developed after fabrication; or
- some 'other feature' that arose in fabrication and/or post-fabrication, including deposition and post-excavation treatment.

Technological decisions

The sandals and six ambiguous sheets display punched holes presumably designed for threading, to facilitate attachment to another material or to enable suspension of the metal. The symmetry of the holes and their occurrence in areas that do not show obvious stress suggest intentional design. They are always found at the sheet's edges and are carefully aligned with each other. They are circular except in the case of S1, which displays rectangular holes, and S2, which has rectangular and elliptical holes. One circular hole on S4 may have been deformed dramatically in subsequent hammering, use, deposition, or post-recovery handling. On all sheets, except S3, the holes have been punched from the same side, identified by the direction of the metal at the edge of the holes (curving inward or outward).

Five ambiguous sheets were embossed, creating a geometric design in low relief. On three (L5, L9, L15) the design was applied on one side, but on the other two (L1, L2) there are raised and depressed areas of the design on a single side, indicating chasing and repoussé were performed. The tools applied to make embossed circles are distinctive: L1 was embossed with a double-pronged tool, L5 with a single-pronged tool and L15 with a single-pronged but bevelled tool. Occasionally, the relief is not entirely symmetrical but deformed, suggesting that insufficient pressure was applied to that point during the original embossing.

One sandal, one axe-money and five ambiguous sheets have an incised guideline near their edge that would have been used as a guide for the metalsmith to follow while cutting the sheet. This guideline is never preserved for the entire perimeter of the object, suggesting that, for the most part smiths carefully followed it, leaving only 'clean' metal in their wake.

Consequences of primary fabrication

Some superficial features may be unintentional products of fabrication. One such feature is porosity, small depressions that developed through the trapping of gases as the metal cooled after melting or annealing. Porosity is highly localized on one sheet but more widely distributed on five sandals and the serpent sheet.

Extra metal is present on two objects as a tab at an edge, and on three as a fine superficial addition. These could have resulted from imprecise cutting or may represent vestiges of metal attachments that have not been preserved, such as ankle attachments to sandals. Ridges are present on the edges of the axe-monies (though they are not as prominent as the 'raised flanges'

Hosler *et al* (1990) identified on other examples) and of four ambiguous sheets. These features developed from hammering the interior regions of the sheets: as these regions thinned, metal moved to edges, thickening them. One ridge (on L16) developed differently: it represents the metal that was displaced when a cutting tool (whose impressions are preserved) was applied to the other side's edge, forming a depression and causing metal to curl over the edge.

Examination of cut edges suggests that varied cutting tools and/or cutting intensities were applied to different objects. Relative assignments of 'smooth', 'rough' and 'very rough' edges were given to each object. Six objects were consistently 'smooth' while one sandal showed 'very rough' edges. Interestingly, different edge areas of individual objects had varying degrees of roughness. This variation may be attributed to preservation or to a decision to cut the object at a later time, applying a cutting tool or intensity different from that originally applied. The tubes, which display smooth edges on their long sides but rough edges on their short sides, may have been cut and rolled and then, at a later time, cut in a different fashion.

Secondary alteration

Torn edges are evident on eight sheets. Intentionality is suggested by the regularity of tears on the sandal and the depth of the tears on one of the other sheets. Tearing may have occurred when the object was removed from the material to which it was attached. The less frequent and less conspicuous tears on other sheets may have developed during their original outlining by cutting, if the metal was especially thin.

Eleven sheets have curled edges. These features could have developed when the object was applied to or removed from its substrate, though on L16 it is related to the object's original cutting. Their presence suggests that the metal overlapped the substrate and perhaps light hammering or burnishing was performed in these curled regions to secure the materials' attachment.

Isolated and amorphous indentations appear on two sheets, neither of which is embossed. These features are reminiscent of depressions seen on cast, high-Au bells.

Other features

Nine sheets have wrinkles on their surfaces that are irregularly oriented and usually clustered. These features may be by-products of hammering and/or embossing but more likely developed if the sheet was crumpled after fabrication. Conservators unravelled crumpled balls of metal in order to study their interiors, potentially adding wrinkles to the sheet (D Piechota pers comm). Five sheets have thin, relatively parallel creases that extend across their long side, and one sandal has a single crease parallel to its short side. The metal may have been rolled and then flattened before deposition or after recovery.

Two sandals, one axe-money, four other sheets and one non-sheet display cracking, which developed during thinning of the metal, in use, induced by the pressure of the foot on the sandal, in the deposit as the metal was compacted by other materials and/or in cleaning and conservation. L15 showed cracking that coincided with a circular design element and would have arisen during the embossing process. Six sheets and the two non-sheets display voids, which are asymmetric and located adjacent to areas of stress, such as wrinkles. The voids formed during hammering of the metal or when the metal was being crumpled or uncrumpled.

Seven objects exhibit incisions (deeper), while nine pieces display striations (lighter). These depressions can be isolated or clustered. Unlike the incised guidelines, these lines are not parallel to cut edges and localized at the edges. While the vastness of some striation clusters may be associated with fundamental hammering of the metal, with the striations following the direction of working, others have developed in the process of embossing geometric designs. The dense cluster of deep incisions on one sandal's ankle strap itself may have served as a 'guideline', potentially made on the sheet before it was cut as a way to delineate the area required for the strap.

All but four of the objects display localized discoloration. Some are fine green circular discolorations that may have arisen in post-excavation cleaning; Lothrop (1915-1962) noted this discolouration as a possible consequence of a nitric acid solution applied to one unidentified Cenote metal. Other discolorations are likely corrosion products.

Composition, distribution and enrichment

Mindful of its limitations (Schulze 2013; Shackley 2011; Shugar 2013), we drew on pXRF data in a limited quantitative extent to form broad compositional groups. A ternary diagram (Fig 9) of all *tumbaga* sheet analyzed (n=70) reveals clusters of high-Au (>90wt%) (n=50) and high-Cu (>85wt%) (n=16) objects. Sandals fall in the high-Cu cluster, but one (S6) shows highly variable composition at multiple points. Unlike the *tumbaga* bells, whose Ag content never exceeded 6wt%, three *tumbaga* sheets have notably higher Ag content, 8wt% (L15), 25wt% (L6) and 26wt% (L5), and plot sepa-

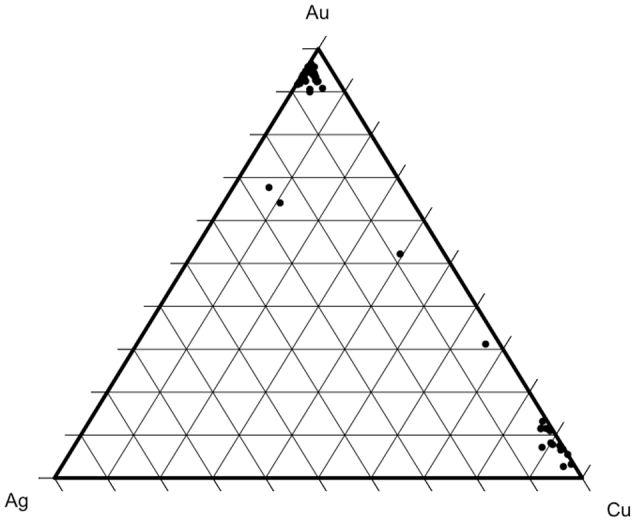

Figure 9: Ternary Au-Ag-Cu diagram for the tumbaga sheets. Each point represents the pXRF analysis of one representative location on each sheet (n=70), including the 18 described in this paper.

rately from the two main clusters in Figure 9. Table 3 presents the compositions of all 22 objects detailed in this paper, in terms of major, minor and trace elements. Among the 18 *tumbaga* sheets, Fe, Zn, Pt and Bi were frequently present. Fe is particularly prominent in L2, where it is more concentrated in reddish areas. Sn is present at significant trace concentrations in L5 and L6. The seven high-Au objects are not ideal for hardening because their compositions fall in the single-phase solid-solution region of the Au-Ag-Cu phase diagram (ASM International 1990, 705-706). Indeed, the three most heavily embossed sheets (L5, L9, L15) have significantly lower Au concentrations. The higher Ag content of the tubes increases their hardness, drawing the ternary alloy into the two-phase region. The axe-monies are primarily Cu with trace As (<1wt% and <1wt%). Arsenic yields a noticeable enhancement in the strength and hardness of Cu starting at concentrations of 0.5wt%; its concentrations in these two objects fall in the range of low-As Cu-As alloys (*c*0.1-0.5wt%) noted by Hosler *et al* (1990, n. 2).

Table 3: Elemental composition of the objects as determined by pXRF.

Object Form	Object-Analysis ID	XRF	Ca	Ti	Cr	Fe	Ni	Cu	Zn	As	Ag	Sn	Pt	Au	Bi	Group
Sandal	S1-1	B				t		M	t	t	t			m		3
	S2-1	B				t	t	M	t	t	t			M		3
	S3-1	B				t	t	M	t	t	m	t		m		3
	S4-9	S				t		M			m					3
	S5-1	S						M			t			m		3
	S6-10	S				t		M			m			M		2
Tubes	L13-5	S			t	t		t			m			M		1
	L14-6	S		t	t	t		t			m			M		1
Ambiguous	L1-2	B				t		m	t		m		m	M	t	1
	L2-2	B				m		m	t		m		m	M	t	1
	L3-1	B				t		m	t		m		m	M	t	1
	L4-3	B				t		m	t		m		m	M	t	1
	L5-1	B				t		m	t		M	t	t	M	t	2
	L6-1	B				t		M	t		M	t	t	M	t	2
	L9-2	S						M								3
	L10-5	S				t		M		t	t			m		3
	L15-1	S	t			t		M			m			M		2
	L16-1	S				t		t			m			M		1
Axe-money	L11-6	S						M		t						3
	L12-6	S						M		t						3
Tweezers	U2-4	S						M	m	t		m				3
	U3-4	S						M	m	t		m				3

Notes: Two different pXRF systems (B = Bruker, S = SANDRA) were used (see Appendix).
One analysis was made at a representative location. Sb and Pb were sought but not detected.
M = major (≥10wt%), m = minor (10>x≥1wt%) and t = trace (<1wt%).
Group: 1 = high-Au, 2 = intermediate composition, 3 = high-Cu.

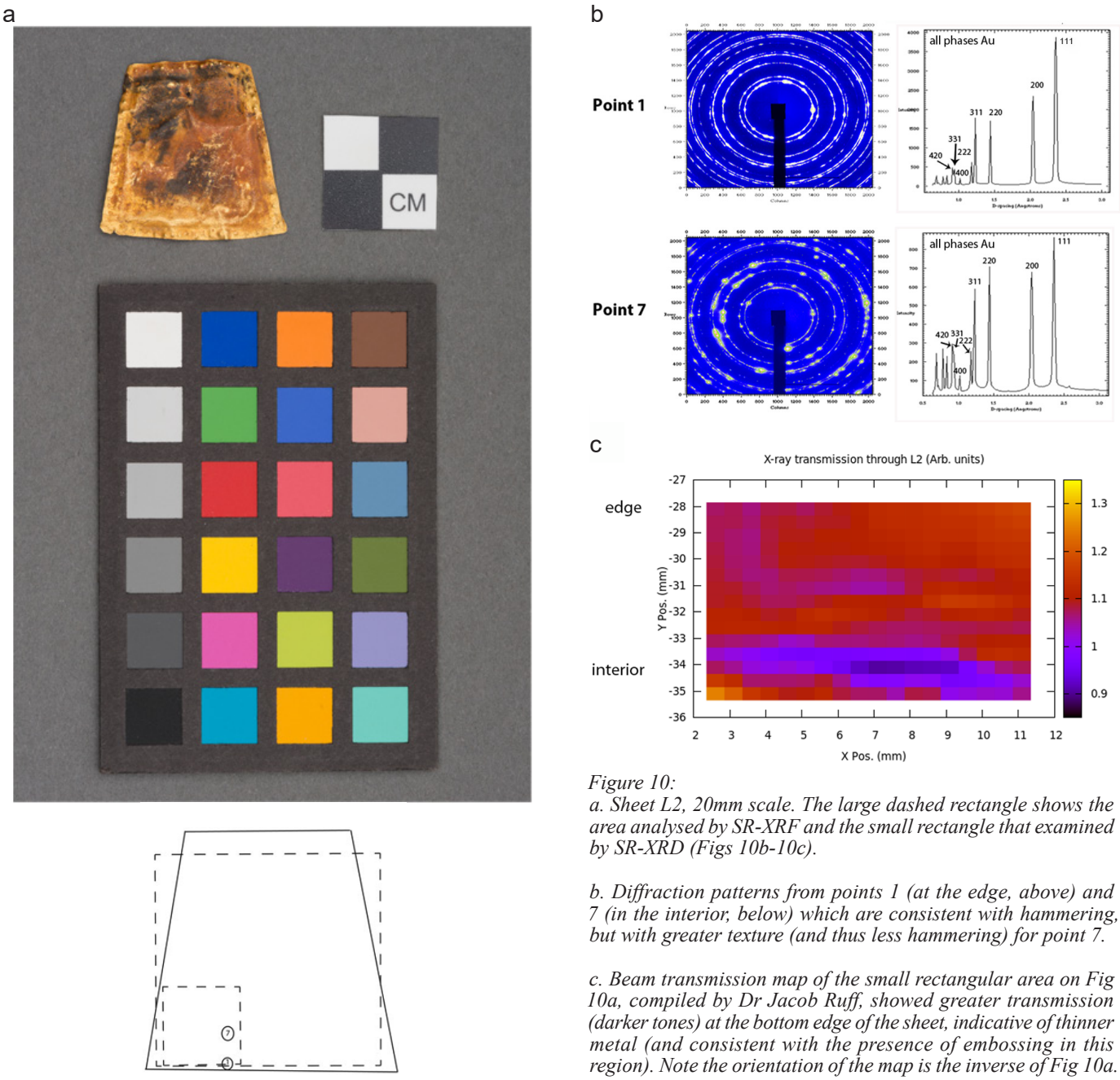

Figure 10:
a. Sheet L2, 20mm scale. The large dashed rectangle shows the area analysed by SR-XRF and the small rectangle that examined by SR-XRD (Figs 10b-10c).

b. Diffraction patterns from points 1 (at the edge, above) and 7 (in the interior, below) which are consistent with hammering, but with greater texture (and thus less hammering) for point 7.

c. Beam transmission map of the small rectangular area on Fig 10a, compiled by Dr Jacob Ruff, showed greater transmission (darker tones) at the bottom edge of the sheet, indicative of thinner metal (and consistent with the presence of embossing in this region). Note the orientation of the map is the inverse of Fig 10a.

SR-XRF revealed the compositional heterogeneity in sheet objects that was less evident using pXRF on its own. The distribution of Au is consistent across the surface of sheet L2, but Fe and Cu are concentrated at the centre and depleted at the edges. While annealing would have gradually oxidized and removed baser elements across the whole surface, the concentration of hammering and annealing at the object's edges, where embossed designs feature, would have accelerated the depletion of Fe and Cu there. Sandal S2 (Fig 11a) was subjected to a surface-wide SR-XRF scan (Fig 11b). While Cu is relatively consistent across the sandal surface, more Ag and especially Au are present along the edges.

Diffraction patterns recorded for four sheets (L2, L3, S2, S3) show fine, continuous rings, indicating that the crystal planes have a randomized orientation that would have been caused by hammering (Figs 10b, 11c). As anticipated for high-Au objects L2 and L3 and high-Cu objects S2 and S3, the phases identified for each object pair, based on peak locations in their intensity *v* d-spacing diagrams, are pure Au and pure Cu, respectively. Diffraction patterns, moving from the edge to more interior points on L2, reveal increasing texture, indicated by a variety of large spots, a result of the preferred orientation of crystal planes. The grains are thus larger near the object's centre. This difference in grain size correlates with the reality that the edges

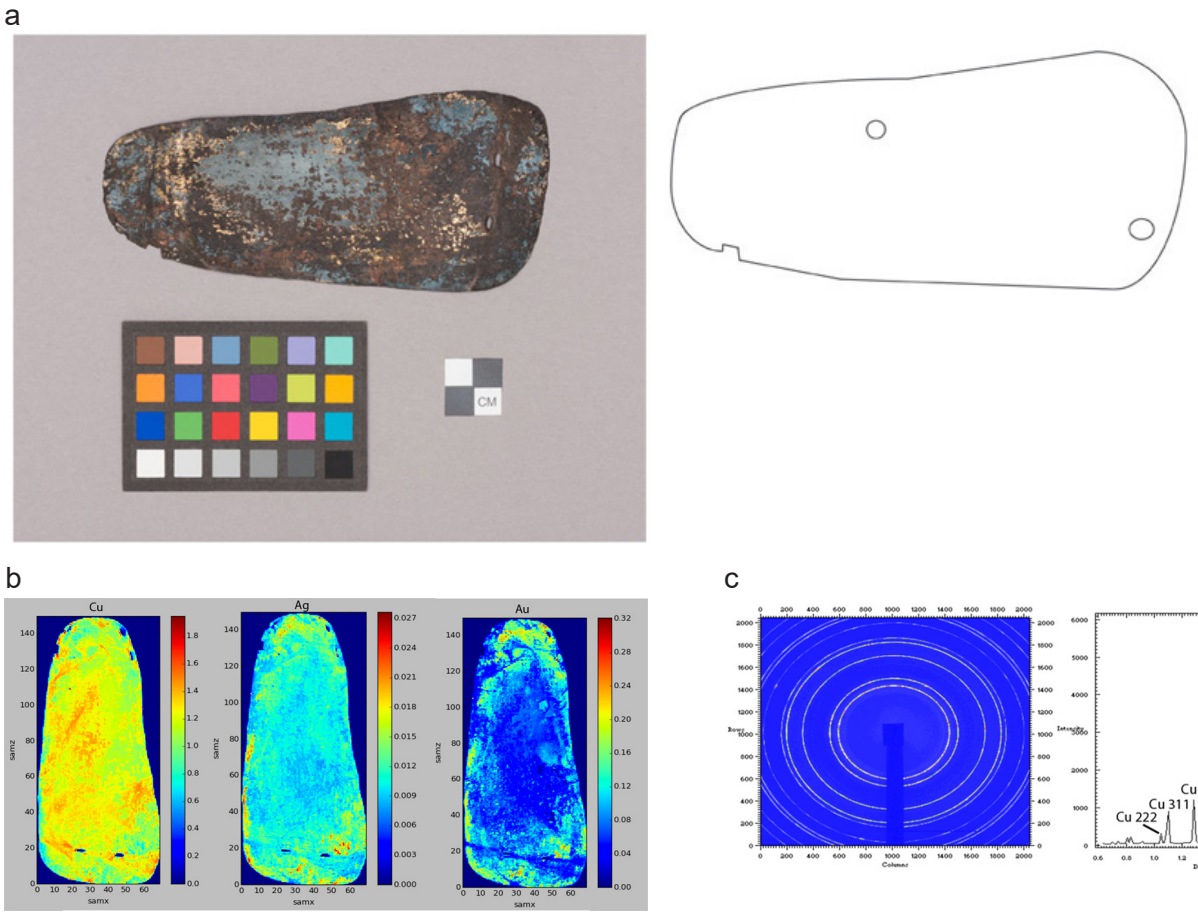

Figure 11:
a. Sandal S2, 20mm scale. SR-XRD analysis made at left circle, RBS analysis at right circle.
b. SR-XRF distribution maps. Lighter tones show higher concentrations of elements; see also front cover.
c. SR-XRD pattern from S2 which is consistent with hammered polycrystalline material. All phases identified were pure Cu.
d. RBS data (He++, 3MeV) modelled with SIMNRA, revealing superficial enrichment in Ag and Au and a pure-Cu substrate, cf Table 4.

Table 4: Modelled composition (wt%) and thickness of surface layers on S2 showing superficial enrichment of gold and silver.

Layer	O	Cu	Ag	Au	Thickness (µm)
1	5.2	66.3	10.1	18.4	0.06
2	4.4	69.7	9.2	16.7	0.07
3	2.6	74.7	8.0	14.7	0.10
4	0.6	83.1	6.3	10.0	0.09
5	0.2	86.4	4.7	8.6	0.15
6	0.4	96.8	2.5	0.3	0.18
7	0.0	100.0	0.0	0.0	118.34

Notes: Data derived from RBS analysis using a 3MeV He++ and modelling with SIMNRA (see Appendix). Layer 1 is at the surface (channel 850) and layer 7 represents the bulk metal (channel 600).

are embossed while the centre of the object is not. While crystal growth, which is temperature-dependent, facilitates texture, the main cause of this feature is likely deformation, given that the texture gradient parallels the embossing gradient. Mapping the diffracting X-ray beam's transmission showed thinner metal in embossed regions than in non-embossed regions (Fig 10c).

While Ag and Au were detected in sandals S2 and S3 by pXRF, the SR-XRD result was interpreted as an indication, given the higher penetration of X-rays in the latter analysis, that Ag and Au are confined to the very surfaces of these objects and RBS confirmed surface enrichment in Ag and Au on sandals S2 and S3 (Fig

11d, Table 4). We thus propose that Ag and Au are not intentional components of the sandals' bulk metal. We simulated superficial enriched layers, the thickness of which is 0.7μm, on each sandal. These results agree with the previous measurements of other Cenote metals by Contreras *et al* (2007). These layers fall within the 0.5-2μm enriched layer thickness that Lechtman *et al* (1982) attribute to electrochemical replacement gilding, where Au (and Ag) from an external source are deposited onto a substrate whose surface pits serve an anodic role before being shut off from the electrolyte (Lechtman *et al* 1982, fig 30). This gilding technique was also detected on other artefacts from the Maya area (Peñuelas *et al* 2012). Although Lechtman *et al* (1982) observed gilding that covers entire surfaces of archaeological objects, the substantial corrosion on the sandals and our inability to remove samples for metallography impeded any determination of the precise composition of the enriched layers across the sandals. Golden patches are scattered on the surface of S2, with greater presence near the edges than the centre, aligning approximately with the high-Au areas revealed by SR-XRF, but there are neither golden nor silvery areas immediately visible on S3. In gilding, the Au and Ag were likely deposited together, so we assume that the variability in Au concentration across the surface, seen in our SR-XRF scan (Fig 11b), was not initially present. While the cause of depletion is more likely to be natural corrosion, following the observation of Scott (1983) of a black powder containing Au in Cu_2O and potentially AgCl on gilded *tumbaga* objects, we should consider that people wearing and/or carrying these sandals may have been aware of these corrosion-induced transformations in colour and lustre, and not render these changes 'invisible' by treating corrosion as solely a post-deposition phenomenon.

On high-Au sheets L2 and L3, we detected superficial Au-based mineralisation and, on L2, we identified Cu-based mineralisation with RBS. These features are again consistent with the findings of Scott (1983), that Au may be particularly subject to corrosion through interaction with certain plants and microorganisms, especially in aquatic environments, and that in *tumbaga* objects Cu-containing (anodic) phases are prone to corrosion, though this is more likely in the presence of superficial enrichment in Au/Ag, due to the drastic differences in electrochemical potential between Cu, Ag and Au.

The contributions of metallurgical communities

The lack of metallurgical evidence related to sheet production in Mesoamerica impedes our ability to place a chronological or geographical frame on the fabrication of the Cenote sheet. The paucity of detail about sheet finds, including qualitative characterizations of attributes like the degree of wrinkling or the roughness of cut edges, poses an additional challenge. However, by identifying patterning across the sheet assemblage and comparing these patterns to known metallurgical traditions, we can begin to evaluate the contributions of different metallurgical communities to the Cenote deposit.

Diagnostic features

Of special note are two hammered, non-sheet objects from the Cenote, which we originally assumed were fragments of anthropomorphic figurines given the similarity of their spiral design elements to those incorporated in the headdresses of certain Cenote figurines. These specimens (U2, U3) are actually fragments of spiral tweezers, separated from their blades. Like those that Hosler (1994) studied, the thickness of the spirals is greater than that of the bridge between them, and the bridge is narrower closer to the blade (or its presumed location). This latter observation is consistent with the reality that, in fabrication, the metal for the spirals is taken from the blade's metal; indeed, these tweezers are fabricated from one strip of metal. On the other hand, the length of each spiral if it was unwound is nearly half of the length Hosler measured and the compositions of the two corpora are different. Both contain trace As (<1wt%) but in addition to lower Sn content (1, 3wt% in the Cenote tweezers compared to ~10wt% in Hosler's examples), the Cenote tweezers also contain Zn (4, 3wt%). If ancient metallurgists sought to enhance working properties, the addition of Sn (at concentrations present in both corpora) improves the metal's springiness, formability and fatigue resistance; the presence of Zn in Cu would enhance its strength and springiness, and the inclusion of Sn or As with Cu-Zn would inhibit dezincification (Davis 2001, 64-65). Hosler (1994) ascribes their fabrication solely to Tarascan metallurgists, who worked between the 14th and 16th century AD. The Zn content, low relative to other European brasses, could represent an intentional alloy; however, it may be a case of 'natural brass', a term used by Craddock (1995) to refer to the presence of Zn up to approximately 6% in axes, chisels, a needle and a plaque from NW Argentina (González 1979). There is no evidence of manufactured brass fabrication in Mesoamerica before the invasion of Europeans (Martinón-Torres *et al* 2007). We therefore propose that the Cenote tweezers were fabricated in west Mexico and, if manufactured brasses, as early as the 16th century AD, drawing on a design that originated in the centuries just before. This low-Zn (and low-Sn) brass

would have been more pink than yellow, a contrast to the 'gold tweezers' [authors' translation] shown as yellowish ornaments worn by priests in the *Relación de Michoacán* (f. 61r), a document written between AD 1539 and 1541 by Friar Jerónimo de Alcalá.

The two axe-monies from the Cenote are also likely to have been fabricated in west Mexico but at an earlier time, probably after AD 1040, when alloy-based metallurgical practices emerge in the region (Hosler 2009). They are identical in form to Type 1a (Hosler *et al* 1990), a type found in Guerrero, Michoacán and Oaxaca, but their length is more similar to those from Guerrero and Michoacán. Their concentrations of As (<1wt%) fall toward the low end of the wide range (0.05–6.35wt%) of As in these Type 1a axe-monies. One of the two shows a corrugated surface, also observed on the published Type 1a axe-monies, a feature that may lend strength to the very thin sheet; raised edges were seen on both, but not to the extent that Hosler *et al* (1990) recorded for other axe-monies from Mexico and Ecuador. We noted massive internal voids on both Cenote axe-monies (Fig 4); a similarly located but less dramatically-sized void is seen in a Type 1a axe-money from Guerrero (Hosler *et al* 1990, fig 6). Considering the surface collection of a stack of 13 Type 1a axe-monies by Weitlaner (reported in Hosler *et al* 1990), we wonder whether these axe-monies were bundled at one time and whether these internal voids, though they are irregular in shape, may have been intentionally created to help thread the objects together.

The two rolled tubes (Fig 5) may be blanks from which other sheet objects, such as beads, were cut, following the hypotheses of Stone and Balser (1958) and Harrison *et al* (2012, 53) for assemblages from Panama. If this interpretation is correct, the raised lines adjacent to one open end of each tube may have served as guides to smiths as they cut metal for the beads. The tubes also may be ear rods that once enveloped wooden or stone substrates. The parallel creases on sheets L3 (Fig 6) and L4 suggest that they were once rolled tubes. Their maximum widths, 42mm and 38mm, compare well with the circumferences of tubes L13 and L14, underestimated due to overlapping metal in each roll, which are 39mm and 38mm, respectively. This similarity, taken with the guideline along one short end of the flat sheet L3, lead us to propose that these sheets could also have been used as blanks for cutting beads or other objects. However, when rolled, L3 and L4, each with a single curvilinear side, would appear differently than would L13 and L14. Alternatively, they may be flattened arm or leg cuffs. The tubular beads, ear rods and cuffs have analogues at Sitio Conte, whose grave sequence begins *c*AD 700 and some of whose metals are housed at the Museum of Fine Arts, Boston (MFA) and the University of Pennsylvania Museum of Archaeology and Anthropology (Penn) (Cooke *et al* 2000; Lothrop 1937). These beads and rods typically have two open ends, occasionally show ridges or guidelines (*eg* MFA 1971.948) at their open ends that suggest cutting and, most interestingly, show indentations (*eg* MFA 1971.932). The indentations on the shorter tubular beads and the longer tubes from which the beads were cut presumably were made after cutting; an alternative is that indentations were made on the longer tubes and then the beads were cut, but the presence of an indentation would seem to impede further cutting. Lothrop (1937) suggests that the sheet used to make the cuffs was 'trimmed to the shape of a truncated triangle' before being rolled; clearly, however, there are also rectangular 'cuffs' from Sitio Conte (*eg* Penn 40-13-93). We propose that the four sheets from Cenote (L3, L4, L13, L14) were fabricated by the metallurgists whose work also has been recovered from Sitio Conte. If we assume the tubes pertain to beads, the presence of cast beads in the Cenote, similar in design and composition to beads from Oaxaca (Camacho-Bragado *et al* 2005), reveals that two bead-making traditions are indicated in the assemblage.

The Cenote sandals lack formal analogues from other regions of the Americas. The enrichment thicknesses on two are consistent with electrochemical replacement gilding, which has been identified on sheet metals from the Moche site of Loma Negra in Peru (Lechtman *et al* 1982; Schorsch *et al* 1996). The account of Díaz del Castillo (1955) of the 16th-century Spanish presence in Mexico mentions that provincial leaders from the Río Grijalva (in present-day Tabasco) brought 'two soles of gold' as tribute (Ch 26) and that the Mexica leader Montezuma II wore 'soles of gold and very precious stonework on top of them' (Ch 88) [authors' translations]. While we cannot assume that golden sandals were necessarily fabricated in the Río Grijalva region, we can propose that sandals, incorporating a technology in use in the Andes in the early-to-mid first millennium AD (Lechtman *et al* 1982), may have reached the Cenote directly or indirectly by means of the Mexica tributary system. We wonder if, despite Díaz del Castillo's characterizations of the sandals as 'of gold', their surface colour was more varied as the Cenote examples were paler, given the distribution of Ag relative to Au we detected on one sandal's surface using SR-XRF (Fig 11b).

Turning to other diagnostic features, Au-Pt alloys are characteristic of La Tolita-Tumaco metal sheet

fabrication (Scott 2011) but Pt concentrations in such objects far exceed those in the Cenote sheets, where Pt is present between <1 and 2wt% (in six objects). As Bray (1974, 39) proposes, such concentrations suggest the Pt was an impurity in the Au source. Minor concentrations of Pt have been reported in a few objects recovered at Panamanian sites, such as El Caño, and, while no Pt has been detected in alluvial Au samples from Costa Rica, trace Pt has been reported in ores from Cerro Colorado and Petaquilla in Panama (Cooke *et al* 2003; Fernández 2010).

Ag concentrations serve as limited diagnostic tools, and the Cenote objects point to Isthmian alluvial Au sources. The high Ag content (≈25wt%) of two otherwise dissimilar sheets (L5, L6) may indicate a vein source (Fernández 2010). Ag was probably a natural component of the Au and, following Uribe and Martinón-Torres (2012), the ratio of Ag to (Ag+Au) can indicate the Ag content within the source material. Figure 12 shows that the overwhelming majority of *tumbaga* hammered objects from the Cenote have a Ag/(Ag+Au) value between 3 and 9%, strikingly different from the Ag/(Ag+Au) distributions of the 210 Muisca objects Uribe and Martinón-Torres studied, which peaked at 15-18%, aligning with the Ag/(Ag+Au) values of Colombian alluvial Au. Recognizing the presence of Cu in alluvial and vein Au sources in Costa Rica (<1% and <2% respectively), Fernández (2010) notes a variable content of Ag (<6% from alluvial sources and <25% from vein sources). Cooke *et al* (2003), recognizing wide ranges of Ag contents in primary materials from Panama, caution against using Ag content diagnostically. The Isthmus offers an array of Cu sources, from which Cu could be alloyed with Au; these include native Cu, chalcopyrite and polymetallic deposits (Cu-Fe-Sn-Pb) in Costa Rica (Fernández and Segura Garita 2004) and native Cu and Cu ores in Panama (Cooke *et al* 2003). We propose that Au was deliberately alloyed with Cu in 38 of the 70 objects whose bulk composition is presented in Figure 9; the other 32 (including tubes L13 and L14 and sheet L16) have trace Cu contents.

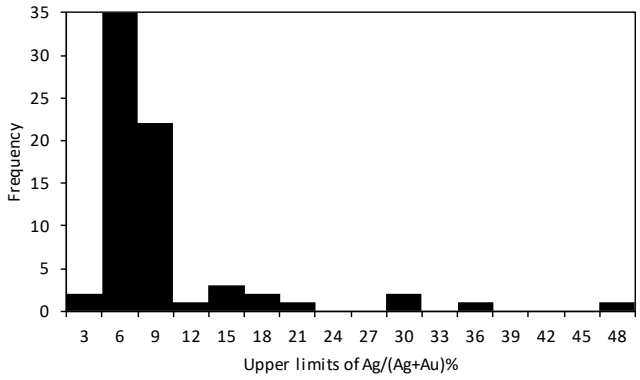

Figure 12: Ag/(Ag+Au) ratios for all hammered tumbaga objects from the Cenote.

Stone and Balser (1958) documented 'punctate' designs (embossed circles) on sheet objects that they connect (whether they imply the objects' place of production or place of deposition is uncertain) to metal corpora from the Zenú region (in Colombia) and the Diquís region (in Costa Rica). One object they photographed bears similarities to sheets L5 and L15 in its rectangular shape and embossed design. These two objects, and L9, may be parts of larger metal sheets and/or products of experiments with punching tools, particularly L9 which is covered with varied embossed designs in different orientations.

Hammering in three dimensions

The Cenote sheet objects are not always flat and two-dimensional. At least two were rolled to form tubes. Four other sheets display some degree of concavity, and sandals, considering the preservation of an ankle strap with one sole, were also conceived in three dimensions. Similarly, secondary design practices, such as punching holes and embossing, gave depth to the sheet. The attachment of metal to a substrate, such as sandal soles to yucca fibre, and the practice of superficial enrichment in Au and Ag were other methods by which metal crafters played with layering. Analysis with pXRF revealed the presence of Cu on three yucca sandal attachments (J Jungels pers comm). Specifically we wonder about the sandals' visual effect: their surface lustre must have been partially concealed, on one side by the yucca support and on the other by the wearer's foot, but still conspicuous enough for Díaz del Castillo to emphasize their gleam.

Crafting parts of wholes

Inherent to the sheets' fabrication is the act of removing a part from a whole through cutting, but further partitioning of the sheet is apparent in the assemblage. The two tubes may have acted as wholes from which parts (hammered beads), whose whereabouts are unknown, were created. Two embossed sheets (L9, L15), whose geometric designs run to the sheets' very edges, may be parts of larger sheets that were cut after embossing. L9 has a composition and surface colours strikingly similar to certain sandals so may represent a re-designed sandal. Each of these acts of sectioning is a renovation, in which the designer(s) became newly aware of the metal's plastic properties.

Learning to smith

Besides the two sheets (L19, L15) whose extensive embossing suggests experimentation with punching, the asymmetry of embossed circles on one sheet or the shallowness of certain circles compared to others indicates that the designers were exploring the consequences of different degrees of force with one punch or of different tools altogether. On certain sheets, the presence of guidelines for cutting reveals the stepwise character of the fabrication process. Franciscan friar Sahagún's *Florentine Codex* (1577) mentions that featherworkers traced lines into metal sheet that was to be cut. Whether featherworkers made the guidelines on the Cenote sheets, we recognize that mapping the design is a crucial first step in smithing. The preservation of these depressions on the archaeological sheets could be unintentional, or it could reflect an intentional decision to maintain a signature of labour.

Conclusions and future work

The assemblage of primarily hammered (mostly sheet) metals shows evidence of original fabrication in the Coclé region (in present-day Panama), dating to before AD 950, and in Guerrero and Michoacán (in west Mexico) after AD 1040. Sandals may have been fabricated and distributed through the Mexica tributary system into the 16th century AD. Tweezers, followed a Tarascan design and, if the Zn-containing metals used are manufactured brasses, they were fabricated after the Spanish invasion. The difference between the objects' fabrication dates and deposition dates may be large. Between their point of original fabrication and deposition in the Cenote, the objects were re-fabricated, whether by indenting, wrinkling, cutting to form beads, or tearing and separating the metal from its substrate. Thus, given the dates of the objects' original fabrication, inferred from their form and technology, and the time required for transit to Chichén Itzá, potentially following indirect routes, these hammered metals were deposited at the Cenote Sagrado in the centuries after the main occupation of Chichén Itzá (AD 750–1050). This confirms the continuity of the Cenote as a sacred location, as noted in Maya and Spanish documents (Tozzer 1957). The hammered objects show formal similarities that metal workers achieved through diverse approaches: many have suspension holes, but their shape is varied; many display embossed circular patterns, but the punches used for these designs are not identical; most are *tumbaga*, but Ag concentrations may be very different. The Cenote Sagrado became an inclusive ritualized deposition, where hammered metal objects with features that are indicators of diverse technological styles were welcome contributions. Post-fabrication alteration of the metals allowed a more extensive community to participate in the practice of metalsmithing.

Characterization of a wider range of embossed Cenote sheets would be useful to further identify similarities and differences in punches. Further application of RBS and SR-XRD to sheets would be fruitful to investigate whether other sandals and other object forms received artificial enrichments. Recognizing that metallographic examination typically requires invasive sampling, we would consider, with clean surfaces, an analysis such as SEM-EBSD as a possible substitute for metallography. This study could then facilitate comparison with assemblages for which metallography has been undertaken, such as foils from Monte Albán, which were cold-worked but lacked signs of a final anneal (Camacho-Bragado *et al* 2005, 23-24). Although this practice alone may not be uniquely indexical of Mixtec metallurgists, smithing techniques may be one of multiple diagnostics of metallurgical communities.

Appendix: Analytical methods

At the PMAE, microscopy involved a Dino-Lite AD413T-12V portable microscope, with digital photography capability, 20 to 200x magnification, and LEDs tuned to 395nm (UV) and 940nm (IR). Higher-resolution visible light study was conducted with a Zeiss OPMI 1 optical microscope with a Lumenera 1-2C digital camera at PMAE Conservation. At the MPC and MNA, this study was performed with an Edmund E-Zoom6V stereoscope with a Nikon Coolpix 4300 digital camera. UV radiation was applied through a 60-W lamp attached to the stereoscope (254nm) or with freestanding ultraviolet lamps UVGL-55 or UVGL-58, offering short- and long-wave UV (254 and 365nm). IR microscopy was undertaken using a Sony NightShot video camera with IR filter for 700-1000nm detection.

At the PMAE a Bruker Tracer III-SD was used for pXRF analysis. Operating conditions were 40kV; 12.30μA; 12mil [300μm] Al + 1mil [25μm] Ti filter; beam at object surface: 5x6.75mm. Fundamental Parameters was used for calibration, and the measurements were subsequently standardized, employing coefficients (Fe, Ni, Cu, Zn, Ag) and offsets (Sn, Au, Pb), with certified reference materials then normalized to 100wt% (Table 5). Multiple points were analyzed on nearly all Cenote metals, studying several faces whenever possible. Each point was analyzed twice, and each analysis lasted 180 live-seconds.

Table 5: Analyses of certified reference materials used to calibrate the pXRF systems.

Standard		Fe	Ni	Cu	Zn	Ag	Sn	Au	Pb
Naval Brass SRM 1107 (NIST)	quoted	0.037	0.098	61.2	37.3	-	1.04	-	0.18
	measured Bruker (n=5)	0.221 ± 0.003	0.148 ± 0.002	58.8 ± 0.0	37.2 ± 0.0		1.15 ± 0.0		0.17 ± 0.01
	measured SANDRA (n=2)	0.133 ± 0.017	0.094 ± 0.132	56.7 ± 2.7	43.0 ± 2.7		0.07 ± 0.09		0.07 ± 0.10
High-Silver L115 (Xcalibur)	quoted	-	-	48	-	52	-	-	-
	measured Bruker (n=5)			44 ± 0.0		52 ± 0.0			
14-kt Au (Xcalibur)	quoted	-	-	24.6	3.9	12.9	-	58.6	-
	measured Bruker (n=5)			22.4 ± 0.1	4.5 ± 0.0	13.3 ± 0.0		54.5 ± 0.2	
900-50	quoted	-	-	5	-	5	-	90	-
	measured SANDRA (n=2)			9.3 ± 8.5		0.5 ± 0.3		90.2 ± 8.3	
Steel 2205 (Bruker)	quoted	66.134	5.396	0.172	-	-	-	-	-
	measured Bruker (n=5)	63.920 ± 0.295	4.868 ± 0.027	0.227 ± 0.005					

Notes: - = element not present in the reference material. Measured values are given as mean ± 1σ.

At the MPC and MNA, pXRF was performed with SANDRA (Sistema de Analisis No Destructivo por Rayos X), developed at IF-UNAM (Ruvalcaba *et al* 2010), with a laptop (beam size=1-1.5mm diam.; heavy elements: 45kV; 0.05mA; 200 live-seconds for each point; 20μm Al + mylar filter; light elements: 35kV; 0.1mA; 300 live-seconds for each point; no filters). An adjustment in the XRF parameters was made for the MNA metals, which were by and large high-Cu (45kV; 0.05mA; 120 live-seconds for each point; mylar filter). Besides SRM 1107, several Cu-Au-Ag references from Degussa (850/40, 850/340, 750/40, 750/130, 900/50) were used to standardize SANDRA. Recognizing the potential overlapping of As Kα and Pb Lα in pXRF spectra, the relative intensities of As Kβ and Pb Lβ were studied as indications of elemental presence or absence.

Drawing on the potential for high collimation and flux of synchrotron X-rays, useful for thick objects, three sheets were analyzed at the Cornell High Energy Synchrotron Source (CHESS) with synchrotron radiation-XRF (SR-XRF) at beamline F3 to produce elemental distribution maps (17keV; beam at object surface = 0.5mm^2). Spectra were fitted using PyMCA software, which uses fundamental parameters. The analysed depth is similar for pXRF and SR-XRF (*c*10μm for Cu and Au and 70μm for Ag), but continuous surface mapping was only possible with SR-XRF. Four sheets were analyzed with transmission synchrotron radiation X-ray diffraction (SR-XRD) (59.3keV; λ=0.207Å; sample-to-detector distance ≈ 843.9mm; beam size = 0.5mm^2 or 1mm^2; collection time = 4, 40 or 400 live-seconds) at CHESS beamline A2. Diffraction patterns were calibrated with CeO_2 powder and analyzed with Fit2D software. Based on the scattering of X-rays by atoms in crystalline materials, SR-XRD helps in the identification of fabrication technique and metal phases. The analysed depth for SR-XRD using a 59.3keV beam may reach 2mm in a Cu-rich alloy and 0.3mm for a Au-rich alloy.

Four sheets were analyzed with RBS at beamline 30 of the Ion Beam Laboratory at SUNY Albany (H^+ and He^{++} beams, 3MeV, beam at object surface ≈ 2mm^2). The total dose applied during each analysis was 2.5μC. A Pt target was used for calibration. Standards L020 and L115 were used (Table 5). Spectra were processed with RUMP and SIMNRA software. The energy and number of ions that are backscattered as the beam interacts with the material ultimately provide compositional information about the surface of the object and aid in the creation of compositional depth profiles. The analysed depth using a H^+ beam is about 10μm; for a He^{++} beam, the analysed depth is reduced to about 3μm, but the depth resolution increases significantly.

Acknowledgments

We express our thanks to: the PMAE and the Consejo de Arqueología, INAH for permission to study the objects and the staff of the PMAE, MPC and MNA for

their support; Steven Shackley, Rosemary Joyce and Ronald Gronsky (UC Berkeley) for generous guidance; Mayra Dafne Manrique Ortega (UNAM-IF) for analytical support; Jannen Contreras and Gabriela Peñuelas (ENCRyM) and Dennis Piechota (UMass Boston) for their conservation expertise and T Rose Holdcraft and Judith Jungels (PMAE) for analysis of *yucca* sandal attachments; William Lanford (Ion Beam Laboratory, SUNY Albany) for support of RBS use; Darren Dale, Ethan Geil, Jacob Ruff and Robert Thorne (CHESS) for support of XRF and XRD use; Bonnie Heras for guidance in hammering experiments; and the anonymous reviewers of this paper along with editor Justine Bayley for their invaluable comments. We extend our thanks to UC MEXUS, the Stahl Endowment at the ARF, UC Berkeley, the Tinker Foundation at the CLAS, UC Berkeley, CONACYT Mexico LN271614, LN279740, PAPIIT UNAM IN110416 and CONACYT CB 239609 for financial support. CHESS is supported by the NSF and NIH/NIGMS via NSF award DMR-1332208.

References

ASM International Handbook Committee 1990, *Properties and selection: Nonferrous alloys and special purpose materials*, *ASM Handbook,* Vol 2 (Materials Park, OH).

Ball J W and Ladd J M 1992, 'Ceramics', in C C Coggins (ed), *Artifacts from the Cenote of Sacrifice, Chichen Itza, Yucatan* (Cambridge, MA), 191-233.

Bray W 1974, *El Dorado: The gold of ancient Colombia* (New York).

Bray W 1977, 'Maya metalwork and its external connections', in N Hammond (ed), *Social process in Maya prehistory: Studies in honour of Sir Eric Thompson* (London), 365-403.

Breglia L 2005, 'Keeping world heritage in the family: A genealogy of Maya labour at Chichen Itza', *International Journal of Heritage Studies* 11, 385-398.

Camacho-Bragado G A, Ortega-Aviles M, Velasco M A and José-Yacaman M 2005, 'A microstructural study of gold treasure from Monte Alban's Tomb 7', *Journal of the Minerals, Metals and Materials Society* 57, 19-24.

Cirerol Sansores M 1940, Descubrimiento de joyas y objetos arqueológicos de los Mayas, en la orilla del 'Cenote Sagrado' de Chichén-Itzá, Informe del Estado de Yucatán 1115-1. Unpublished but submitted to the Mexican government.

Cobos R 1998, 'Chichen Itza y el Clásico Terminal en las Tierras Bajas Mayas', in J P Laporte and H Escobedo (eds), *XI Simposio de Investigaciones Arqueológicas en Guatemala, 1997* (Guatemala), 915-930.

Cobos R 2010, 'Más allá del centro de Yucatán: Reconstruyendo el dominio territorial de Chichén Itzá en las Tierras Bajas Maya del Norte', in E Ortiz Díaz (ed), *VI Coloquio Pedro Bosch Gimpera: Lugar, Espacio y Paisaje en Arqueología: Mesoamérica y Otras Áreas Culturales* (Mexico City), 333-348.

Cockrell B, Ruvalcaba Sil J L and Ortiz Díaz E 2015, 'For whom the bells fall: Metals from the Cenote Sagrado, Chichén Itzá', *Archaeometry* 57(6), 977-995.

Coggins C C and Shane III O C (eds) 1984, *Cenote of Sacrifice: Maya treasures from the sacred well at Chichén Itzá* (Austin, TX).

Contreras J, Ruvalcaba Sil J L and Arenas Alatorre J 2007, 'Non-destructive study of gilded copper artifacts from the Chichén-Itzá cenote', in J Miranda (ed), *Proceedings of Particle Induced X-ray Emission and its Analytical Applications, PIXE 2007* (Puebla), PI-48, 1-4.

Cooke R, Sánchez Herrera L A and Udagawa K 2000, 'Contextualized goldwork from 'Gran Coclé', Panama', in C McEwan (ed), *Precolumbian gold: Technology, style and iconography* (London), 154-176.

Cooke R, Isaza I, Griggs, J, Desjardins B and Sánchez L A 2003, 'Who crafted, exchanged, and displayed gold in Pre-Columbian Panama?', in J Quilter and J W Hoopes (eds), *Gold and power in ancient Costa Rica, Panama, and Colombia* (Washington, DC), 91-158.

Craddock P T 1995, *Early metal mining and production* (Washington, DC).

Davis J R 2001, *ASM specialty handbook: copper and copper alloys* (Materials Park, OH).

Díaz del Castillo B 1955, *Historia verdadera de la conquista de la Nueva España* (Buenos Aires).

Fernández P 2010, 'Metalurgia de Costa Rica: Producción local e identificación de relaciones sociales entre Panamá, Costa Rica y Nicaragua', *Society for American Archaeology* (St Louis, MO).

Fernández P and Segura Garita J 2004, 'La Metalurgia del Sureste de Costa Rica: Identificación de producciones locales basadas en evidencia tecnológica y estilística', in A Perea, I Montero and Ó García-Vuelta (eds), *Tecnología del oro antiguo: Europa y América* (Madrid), 49-61.

Fleming S 1992, 'Sitio Conte goldworking techniques: Hammering and casting', in P Hearne and R J Sharer (eds), *River of gold: Precolumbian treasures from the Sitio Conte* (Philadelphia, PA), 48-53.

Franco Velázquez F and de Grinberg D M K 2002, 'Cascabeles especiales procedentes del Cenote Sagrado de Chichén-Itzá, Yucatán', in M I R Vázquez Balderas (ed), *Memorias: Mesa redonda: Tecnologías metalúrgicas en América prehispánica* (Mexico City), 17-32.

González A R 1979, 'Pre-Columbian metallurgy of northwest Argentina', in E P Benson (ed), *Pre-Columbian metallurgy of South America* (Washington, DC), 133-202.

Harrison A, Cullen Cobb K, Beaubien H F, Jett P and Mayo J 2012, 'A study of pre-Columbian gold beads from Panama', in N Meeks, C Cartwright, A Meek and A Mongiatti (eds), *Historical technology, materials and conservation: SEM and microanalysis* (London), 49-55.

Hosler D 1988, 'Ancient West Mexican metallurgy: A technological chronology', *Journal of Field Archaeology* 15, 191-217.

Hosler D 1994, *The sounds and colors of power* (Cambridge, MA).

Hosler D 2009, 'West Mexican metallurgy: Revisited and revised', *Journal of World Prehistory* 22, 185-212.
Hosler D, Lechtman H and Holm O 1990, *Axe-monies and their relatives* (Washington, DC).
Lave J and Wenger E 1991, *Situated learning: Legitimate peripheral participation* (New York).
Lechtman H 1984, 'Andean value systems and the development of prehistoric metallurgy', *Technology and Culture* 25, 1-36.
Lechtman, H 2007, 'The Inka, and Andean metallurgical tradition', in R L Burger, C Morris and R Matos Mendieta (eds), *Variations in the expression of Inka power* (Washington, DC), 313-55.
Lechtman H, Erlij A and Barry Jr. E J 1982, 'New perspectives on Moche metallurgy: Techniques of gilding copper at Loma Negra, Northern Peru', *American Antiquity* 47, 3-30.
Lothrop S K 1915-1962, Untitled [and unpublished reports] in Samuel K Lothrop Papers 996-20: Box 3, Folder 10 (Peabody Museum of Archaeology and Ethnology, Cambridge, MA).
Lothrop S K 1937, *Coclé: An Archaeological Study of Central Panama; Part I: Historical background, excavations at the Sitio Conte, artifacts and ornaments* (Cambridge, MA).
Lothrop S K 1952, *Metals from the Cenote of Sacrifice, Chichen Itza, Yucatan* (Cambridge, MA).
Martinón-Torres M, Valcárcel Rojas R, Cooper J and Rehren T 2007, 'Metals, microanalysis and meaning: a study of metal objects excavated from the indigenous cemetery of El Chorro de Maíta, Cuba', *Journal of Archaeological Science* 34(2), 194-204.
Ortiz Díaz E, Cockrell B and Ruvalcaba Sil J L 2016 'Las distintas tradiciones metalúrgicas presentes en las ofrendas del Cenote Sagrado de Chichén Itzá', *Arqueología Mexicana* 23(138), 72-74.
Pendergast D M 1962, 'Metal artifacts in Prehispanic Mesoamerica', *American Antiquity* 27, 520-545.
Peñuelas G, Jimenez I, Tapia P, Ruvalcaba-Sil J L, Arenas J, Lemoine A, Contreras J, Ruiz Portilla P, Rivero Torres S, 2012, 'Technical study of a set of metallic artifacts from the Maya site of Lagartero, Chiapas, Mexico', *Materials Research Society Symposium Proceedings* 1374, 125-136.
Piña Chán R 1970, *Informe preliminar de la reciente exploración del Cenote Sagrado de Chichén Itzá* (Mexico City).
Root W C 1937, 1946-7, Untitled [and unpublished reports] in William Campbell Root Papers 1932, 1969, 969-42: Box 1, Folders 12 and 13; Box 4a (Peabody Museum of Archaeology and Ethnology, Cambridge, MA).
Ruvalcaba J L, Ramirez D, Aguilar V, Picazo F, 2010, 'SANDRA: A portable XRF system for the study of Mexican cultural heritage', *X-ray Spectrometry* 39, 338-345.
Schorsch D, Howe E G and Wypyski M T 1996, 'Silvered and gilded copper metalwork from Loma Negra', *Boletín del Museo del Oro* 41, 145-163.
Schulze N 2013, 'How "real" does it get? Portable XRF analysis of thin-walled copper bells from the Aztec Templo Mayor, Tenochtitlán, Mexico', in A N Shugar and S E Simmons (eds), *Archaeometallurgy in Mesoamerica: Current approaches and new perspectives* (Boulder, CO), 203-226.
Scott D A 1983, 'The deterioration of gold alloys and some aspects of their conservation', *Studies in Conservation* 28, 194-203.
Scott D A 2011, 'The La Tolita-Tumaco culture: Master metalsmiths in gold and platinum', *Latin American Antiquity* 22, 65-95.
Shackley M S 2011, 'An introduction to X-ray fluorescence (XRF) analysis in archaeology', in M S Shackley (ed), *X-ray fluorescence spectrometry (XRF) in geoarchaeology* (New York), 7-44.
Shugar A N 2013, 'Portable X-ray fluorescence and archaeology: Limitations of the instrument and suggested methods to achieve desired results', in R A Armitage and J H Burton (eds), *Archaeological chemistry* 8 (Washington, DC), 173-193.
Stone D and Balser C 1958, *The aboriginal metalwork in the Isthmian region of America* (San José, CA).
Tozzer A M 1957, *Chichen Itza and its Cenote of Sacrifice: A comparative study of contemporaneous Maya and Toltec* (Cambridge MA).
Uribe Villegas M A and Martinón-Torres M 2012, 'Composition, colour and context in Muisca votive metalwork (Colombia, AD 600-1800)', *Antiquity* 86, 772-791.

The authors

José Luis Ruvalcaba Sil is Professor and Research Scientist at the Instituto de Física at the Universidad Nacional Autónoma de México. He has undertaken archaeometric research on diverse pre-Hispanic archaeological materials, from metals to pigments to greenstone. Since 2014, he has been the head of the National Laboratory of Sciences for Research and Conservation of Cultural Heritage (LANCIC).
Address: Instituto de Física, Universidad Nacional Autónoma de México, Circuito de la Investigación Científica, Ciudad Universitaria CP 04510 México, DF
Email: sil@fisica.unam.mx

Bryan Cockrell is a Curatorial Fellow at the Metropolitan Museum of Art, working on the interpretation of metalwork from Central and South America. Critical of his position as a white settler and of the extractive projects in which archaeology participates, he wants to collaboratively create a world without borders or prisons.
Address: The Metropolitan Museum of Art, 1000 5th Avenue, New York, NY 10028
Email: bryan.cockrell86@gmail.com

Edith Ortiz Díaz is Professor and Archaeologist at the Instituto de Investigaciones Antropológicas at the Universidad Nacional Autónoma de México. She has conducted pre-Hispanic and historical research in the Sierra Norte of Oaxaca and also has studied metallurgy in ancient Mexico.
Address: Instituto de Investigaciones Antropológicas, Universidad Nacional Autónoma de México, Circuito Exterior, Ciudad Universitaria CP 04510 México, DF
Email: edithd@unam.mx